Finite-temperature phase transition of SU(3) gauge theory on Nt=4 and 6 lattices

Finite-temperature phase transition of SU(3) gauge theory on $N_t = 4$ and 6 lattices

Y. Iwasaki, K. Kanaya, and T. Yoshié
Institute of Physics, University of Tsukuba, Ibaraki 305, Japan

T. Hoshino and T. Shirakawa
Institute of Engineering Mechanics, University of Tsukuba, Ibaraki 305, Japan

Y. Oyanagi
Department of Information Science, University of Tokyo, Tokyo 113, Japan

S. Ichii
National Laboratory for High Energy Physics, Ibaraki 305, Japan

T. Kawai
Department of Physics, Keio University, Yokohama 223, Japan

The deconfining finite-temperature transition of SU(3) gauge theory is studied on the dedicated parallel computer QCDPAX. Monte Carlo simulations are performed on $12^2 \times 24 \times 4$, $24^2 \times 36 \times 4$, $20^3 \times 6$, $24^3 \times 6$, and $36^2 \times 48 \times 6$ lattices with 376 000 to 1 112 000 iterations. The finite size scaling behavior of the first-order transition is confirmed both on the $N_t = 4$ and $N_t = 6$ lattices and clear two-phase structures are observed on spatially large lattices ($24^2 \times 36 \times 4$ and $36^2 \times 48 \times 6$). The latent heat at the deconfining transition is estimated both by a direct measurement of the gap on the spatially large lattices and by applying a finite-size scaling law. The results obtained by these two independent methods are remarkably consistent with each other on both the $N_t = 4$ and 6 lattices. The latent heat for $N_t = 6$ is much smaller than that for $N_t = 4$ and is about $\frac{1}{3}$ of the Stefan-Boltzmann value $8\pi^2/15$. The details of the data and the error analysis are presented.

PACS number(s): 11.15.Ha, 12.38.Gc, 12.38.Mh

I. INTRODUCTION

Determination of the nature of the finite-temperature deconfining transition of QCD is an issue of essential importance in understanding the development of the early Universe and in the study of heavy-ion collisions. Recently it has been realized that the determination of the nature of the transition requires much more intensive numerical calculations than done previously even in pure SU(3) gauge theory [1]. Through the recent simulations on the $N_t = 4$ lattices [2–5], with N_t being the lattice size in the temporal direction, the order of the phase transition has now been definitely determined to be of first order. A large spatial volume of lattice as well as high statistics are required both to see a clear first-order signal and to fix the order of the transition by the study of finite-size scaling (FSS) properties. It has also turned out that the latent heat estimated on a spatially large $N_t = 4$ lattice is much smaller than previously determined [2].

In this paper, we study the deconfining transition in pure SU(3) gauge theory first on the $N_t = 4$ system ($12^2 \times 24 \times 4$ and $24^2 \times 36 \times 4$ lattices [6]) with statistics which is largely improved compared with previous works. The results for $N_t = 4$ are completely consistent with previous results. The high statistics of the data enables us to obtain new results such as a clear four-peak

structure of the Polyakov loop at the deconfining temperature. We are also able to perform reliable error analyses of physical quantities because of these high statistics. Then we further study the $N_t = 6$ system ($20^3 \times 6$, $24^3 \times 6$, and $36^2 \times 48 \times 6$ lattices) in high statistics. In order to achieve a quality of the data indicating a clear first-order signal, the spatial size of the lattice as well as the statistics must be enlarged compared with the $N_t = 4$ system. We find that we need the linear spatial extension N_s of the lattice to be at least six times N_t both for $N_t = 4$ and 6 in order to obtain a clear two-phase signal. We present the details of the data and the error analyses for both cases of $N_t = 4$ and 6 systems.

As is shown in detail later, we confirm the FSS of the first-order transition both for $N_t = 4$ and 6 and thereafter determine the latent heat for $N_t = 4$ and 6 both by high-statistics measurement on large lattices and by applying a FSS law. The results obtained by these two independent methods are remarkably consistent with each other both for $N_t = 4$ and 6. We find that the latent heat for $N_t = 6$ is much smaller than that for $N_t = 4$ and is about $\frac{1}{3}$ of the Stefan-Boltzmann value $8\pi^2/15$. A part of this work has been briefly reported in Ref. [7].

In Sec. II, the parallel computer QCDPAX is introduced. In Sec. III, we describe our Monte Carlo runs and discuss the quality of our data. A finite-size scaling analysis of susceptibilities is presented in Sec. IV. Section

V is devoted to the study of the latent heat. Our conclusion is given in Sec. VI.

II. QCDPAX

The simulation is performed on the QCDPAX [8], a massively parallel dedicated computer constructed at the University of Tsukuba as the fifth generation of PAX (parallel array experiment) computers [9]. The QCDPAX project started in 1987 as a joint collaboration of physical and computer science groups mainly at the University of Tsukuba. The machine was designed by the QCDPAX Collaboration for the simulation in lattice QCD and manufactured by Anritsu Corporation.

The global architecture of QCDPAX is given in Fig. 1. QCDPAX is local memory MIMD (multiple instruction multiple data) machine which consists of identical processing units (PU's) mutually interconnected in a toroidal two-dimensional nearest-neighbor mesh. In the spring of 1990, 480 PU's were installed achieving the peak speed of 14 GFLOPS (10^9 floating-point operations per second). Most simulations are performed with 432 PU's to reserve PU's for replacing broken ones. In this case the peak speed is about 12.5 GFLOPS. These peak speeds are confirmed by the square sum calculation $S = \sum_i x_i^2$. We have several *small* QCDPAX's consisting of 16 PU's for the development of application programs and for simulations on small lattices.

Each PU is an independent one-board microprocessor with peak speed of about 30 MFLOPS. It works completely asynchronously with an independent clock. The CPU is Motorola's 68020 and the FPU (floating-point processing unit) is L64133 by LSI Logic company. A specially designed controller FPUC (FPU controller) to operate the FPU in a vectorized way is manufactured using gate-array technology. As the main local memories, each PU has 4 MByte 100 nsec DRAM's (dynamic random access memories) where the program and some intermediate data are stored, and 2 MByte 35 nsec CMOS (complementary metal-oxide semiconductor) SRAM's (static random access memories) where the floating-point
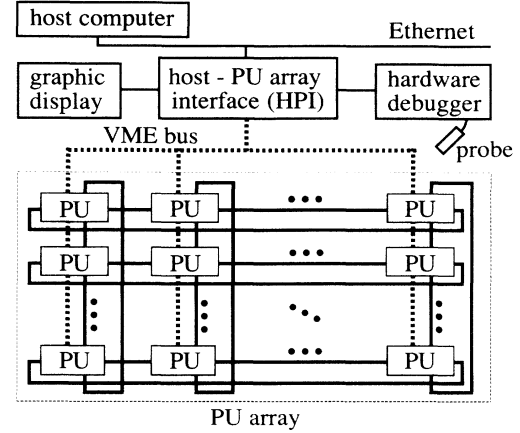

FIG. 1. The system configuration of QCDPAX.

data for the vectorized calculation is stored. The PU array is connected to the host workstation, Sun-3/260, which compiles and assembles the source program, loads the object program into the PU array, initiates parallel tasks, and transfers and receives the data to and from the PU array.

The user of the QCDPAX should prepare two programs: one for the host computer and the other for the PU's. The program for the host computer is written in C. The PU program is written in a newly developed language PSC (parallel scientific C), an extension of C, which has the ability to handle the parallel processing features of the QCDPAX and to perform the vectorized computations with the FPU. A PSC program is compiled to a code in an assembly language qfa (quick floating assembler) which is specially designed for our PU. Optimization of the code can be done at the level of qfa. A compiler and an assembler are developed for coding the PU programs.

Simulations on the $24^2 \times 36 \times 4$ and $36^2 \times 48 \times 6$ lattices are performed on the QCDPAX with 432 PU's, while those on the $12^2 \times 24 \times 4$ and $24^3 \times 6$ lattices are per-

TABLE I. Parameters of the Monte Carlo runs and averages of observables over the full runs after thermalization. Errors are estimated using the jackknife method with the bin size given in the table.

Lattice	$24^2 \times 36 \times 4$	$12^2 \times 24 \times 4$	$36^2 \times 48 \times 6$	$24^3 \times 6$	$20^3 \times 6$
β	5.6925	5.6915	5.8936	5.89	5.8922
Total number of iterations	712 000	910 000	1 112 000	480 000	376 000
Thermalization	2000	20 000	12 000	5000	6000
Bin size	35 500	10 000	50 000	25 000	18 500
Ω_{rot}	0.0680(70)	0.0807(16)	0.0287(24)	0.0305(17)	0.0396(17)
$|\Omega|$	0.0687(69)	0.0818(16)	0.0291(23)	0.0312(16)	0.0402(17)
P	0.549 59(24)	0.549 748(65)	0.581 249(23)	0.580 786(20)	0.581 172(24)
P_s	0.549 38(22)	0.549 503(59)	0.581 224(20)	0.580 761(18)	0.581 138(21)
P_t	0.549 80(26)	0.549 993(71)	0.581 274(25)	0.580 810(21)	0.581 206(26)
$\chi(\Omega_{rot})/V$	$2.079(69) \times 10^{-3}$	$1.935(34) \times 10^{-3}$	$3.43(13) \times 10^{-4}$	$3.52(12) \times 10^{-4}$	$4.07(14) \times 10^{-4}$
$\chi(P)/V$	$2.856(58) \times 10^{-6}$	$5.305(64) \times 10^{-6}$	$7.85(15) \times 10^{-8}$	$2.571(27) \times 10^{-7}$	$4.265(35) \times 10^{-7}$

formed with 288 PU's. The $20^3 \times 6$ lattice is simulated on a small QCDPAX with 16 PU's. Many routines for checking the hardware of the QCDPAX are developed and included in the simulation jobs [6]. About 15–20 % of the total computation time is devoted to these self-checks and recalculations in case of errors. The one link update time, excluding the self-checks, is measured to be 1.44(1.60)μsec on the QCDPAX with 480(432) PU's.

III. MONTE CARLO RUNS AND QUALITY OF THE DATA

We use the standard one-plaquette action

$$S = -\frac{\beta}{6} \sum_p \mathrm{Tr}(U_p + U_p^\dagger) , \tag{3.1}$$

with U_p being the ordered product of the link variables U_l around a plaquette p and $\beta = 6/g^2$. The partition function is defined by $Z = \int \prod_l dU_l \exp(-S)$. Gauge configurations are updated with a three SU(2) subgroup eight-hit pseudo-heat-bath algorithm: a Cabibbo-Marinari algorithm [10] slightly modified for vector processors [11]. The acceptance rate is about 95%.

Parameters of our Monte Carlo runs are summarized in Table I. An ordered initial configuration is used except for the case of the $36^2 \times 48 \times 6$ lattice, for which the configuration obtained with 88 000 iterations at $\beta = 5.895$ from the ordered start is used as the initial one. As is shown below, the values of β's listed in Table I exactly agree with the deconfining transition points β_c within statistical errors except for the case of the $24^3 \times 6$ lattice, on which the value of β is slightly smaller than our estimation of β_c. Our statistics is much improved over the previous works. See Refs. [3–7] for the $N_t = 4$ case. For the $N_t = 6$ case, Brown et al. [2] reported the results of 10 000 to 100 000 iterations at several values of β on $(16^3 – 24^3) \times 6$ lattices. Our spatial lattice size is greatly enlarged and the statistics is one order improved.

At every iteration, we measure the average spatial plaquette P_s and temporal plaquette P_t,

$$P_s = \frac{1}{3VN_t} \sum_{p=\text{spatial}} \frac{1}{3} \mathrm{Re}\, \mathrm{Tr} U_p , $$
$$P_t = \frac{1}{3VN_t} \sum_{p=\text{temporal}} \frac{1}{3} \mathrm{Re}\, \mathrm{Tr} U_p , \tag{3.2}$$

and a spatially averaged timelike Polyakov loop,

$$\Omega = \frac{1}{V} \sum_x \frac{1}{3} \mathrm{Tr} \left[\prod_{t=1}^{N_t} U_{x,t;4} \right] , \tag{3.3}$$

where V is the spatial volume of the lattice. The order parameter for the deconfining transition of SU(3) gauge theory is given by the Polyakov loop Ω, which detects the spontaneous breakdown of the center $Z(3)$ global symmetry at the deconfining transition [12]. In the study of the deconfining transition on a finite lattice, it is convenient to study the $Z(3)$-rotated Polyakov loop $z\Omega$ where Ω is multiplied by an element z of $Z(3)$ such that $\arg(Z\Omega) \in (-\pi/3, \pi/3]$. We denote the real part of $z\Omega$ as Ω_{rot}. To investigate the nature of the transition more

precisely, we also study the susceptibility of Ω_{rot} and the averaged plaquette $P \equiv (P_s + P_t)/2$:

$$\chi(\mathcal{F}) \equiv V \times (\langle \mathcal{F}^2 \rangle - \langle \mathcal{F} \rangle^2) , \tag{3.4}$$

where $\mathcal{F} = \Omega_{\text{rot}}, P$. The expectation values of these quantities are listed in Table I.

We see many flip-flops in the histories of P on all the lattices we have simulated (Fig. 2). The history of Ω
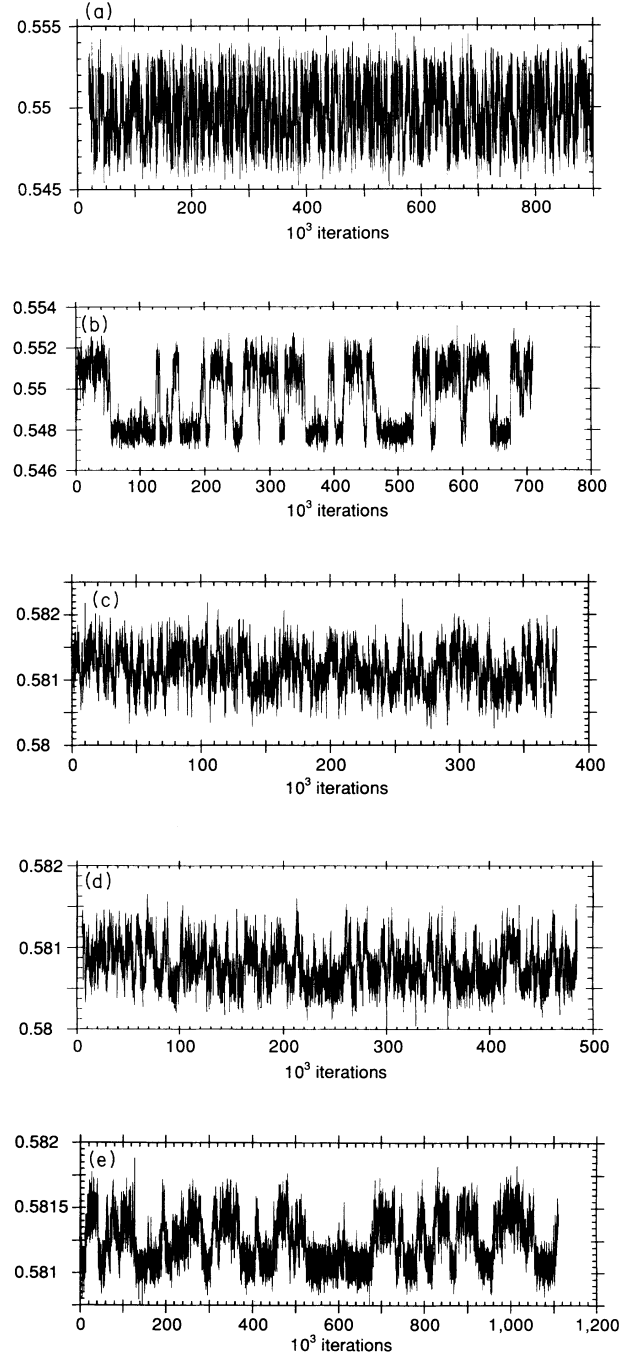

FIG. 2. Time history of the average plaquette P in bins of 100: (a) $12^2 \times 24 \times 4$, (b) $24^2 \times 36 \times 4$, (c) $20^3 \times 6$, (d) $24^3 \times 6$, (e) $36^2 \times 48 \times 6$.

shows clear flip-flops at the same places as that of P. On the spatially large lattices ($24^2 \times 36 \times 4$ and $36^2 \times 48 \times 6$), the histogram of $|\Omega|$ shows a clear double-peak structure and the histogram of Ω on the complex plane a four-peak structure (see Figs. 3 and 4) [13]. Note that the double peaks of the histograms become sharper with increasing V. This implies that the transition is a first-order transition associated with the spontaneous breakdown of the $Z(3)$ symmetry [14]. However, a clearer confirmation of the order of the transition requires a FSS study.

On the $24^2 \times 36 \times 4$ lattice, we find a clear double-peak structure also in the histogram of P [Fig. 5(a)]. On the other lattices, the plaquette histogram has only one peak if we do not bin the data. A bin size of about 100 is required to get a double-peak structure on the $36^2 \times 48 \times 6$ lattice [Fig. 5(b)], while on our small lattices the required bin size is larger than 1000. We note that, in many observables, the separation of the two phases is less clear on the $36^2 \times 48 \times 6$ lattice than on the $24^2 \times 36 \times 4$ lattice. Two possible origins of this difference are (1) the relative spatial volume $V/N_t^3 = 288$ for the $36^2 \times 48 \times 6$ lattice is slightly smaller than the value 324 for the $24^2 \times 36 \times 4$ lattice and (2) as is shown in the following, the deconfining transition for $N_t = 6$ is weaker than that for $N_t = 4$.

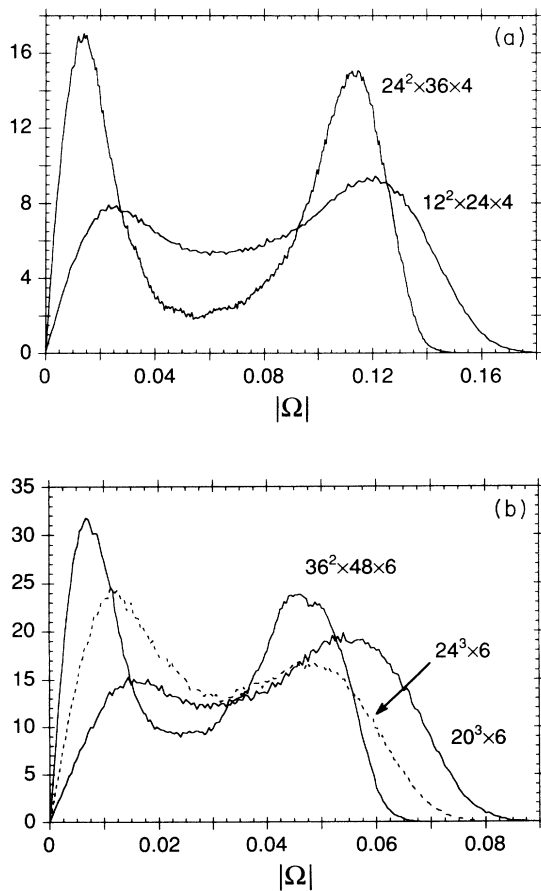Errors are estimated by the jackknife method [15]. To take into account the autocorrelation effects of successive Monte Carlo iterations, we divide the total iterations into bins of a fixed number of successive iterations (bin size) and apply the jackknife method [16]. Bin size dependence of the estimated errors is studied to remove the autocorrelation effects. The large statistics of our data al-
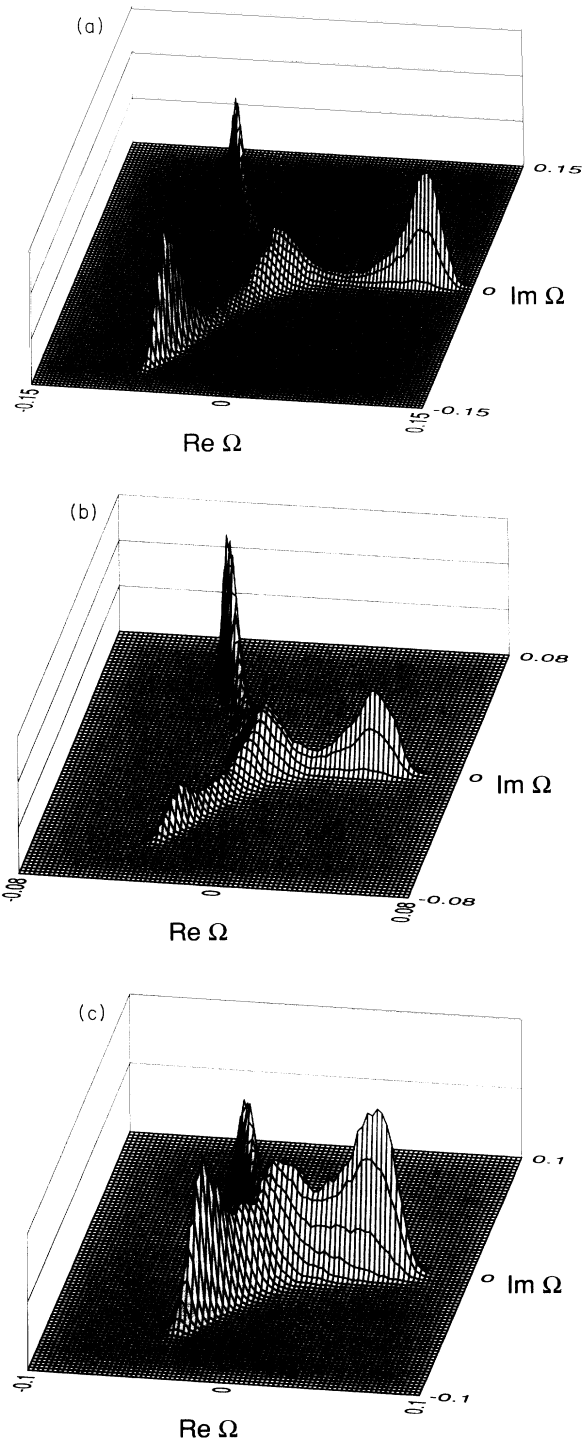

FIG. 3. Polyakov-loop histogram for $|\Omega|$: (a) $N_t = 4$, (b) $N_t = 6$. The normalization is chosen so that the total area becomes unity.

FIG. 4. Histogram of Ω on the complex plane: (a) $24^2 \times 36 \times 4$, (b) $36^2 \times 48 \times 6$, (c) $24^3 \times 6$.
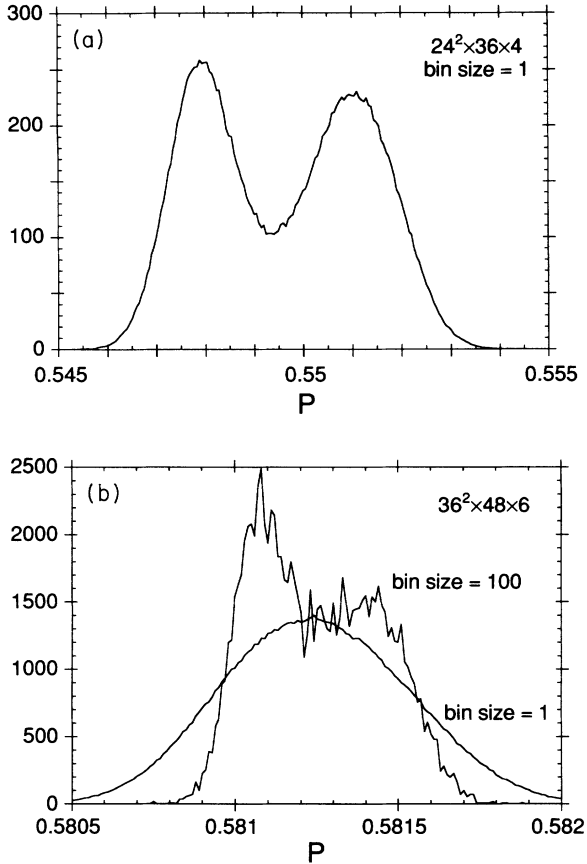
FIG. 5. Plaquette histogram: (a) $24^2 \times 36 \times 4$, (b) $36^2 \times 48 \times 6$. The normalization is chosen so that the total area becomes unity.

lows us to vary the bin size widely. Figure 6 is an example of the bin-size dependence of estimated errors. From such studies of various quantities we find that a large number is required for the bin size to obtain reliable values of errors which are stable under the increase of the bin size. The bin sizes which we use for an error estimation of the observables averaged over both phases are
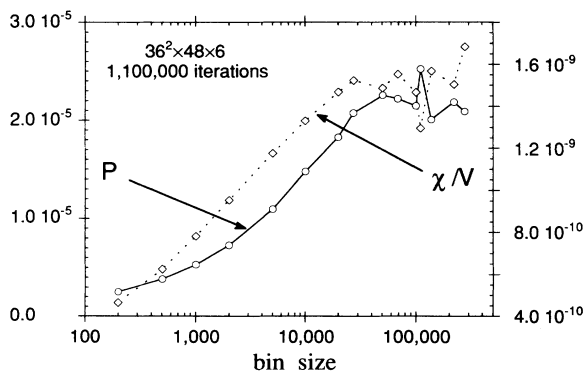

FIG. 6. Estimated errors for the averaged plaquette P and its susceptibility on the $36^2 \times 48 \times 6$ lattice as a function of the jackknife bin size.

summarized in Table I. As expected, these bin sizes are comparable with the average persistent time of the phases seen in the histories, typically 10 000–50 000. For quantities in each phase such as the energy density in the high- (low-) temperature phase, the required bin size is smaller, typically 3000–10 000.

IV. FINITE-SIZE SCALING

The many flip-flops seen in the histories allow us to apply the spectral density method [17] to see the β dependence of the observables near the simulation point. The main purpose of this analysis is to obtain the precise location and properties of the phase transition. In Fig. 7, we show $\langle \Omega_{\text{rot}} \rangle$ as a function of β. The results for the susceptibilities of Ω_{rot} and P are shown in Figs. 8 and 9, respectively. The peak position of susceptibilities provides a finite-volume estimate of the transition point $\beta_c(N_t, V)$, while the peak height χ_{max} of susceptibilities provides us with a useful test of the FSS. Table II summarizes our results for the peak height χ_{max}/V and the peak position $\beta_c(N_t, V)$. Note that our β's for the Monte Carlo runs are located exactly at the transition point within the errors except for the case of the $24^3 \times 6$ lattice.

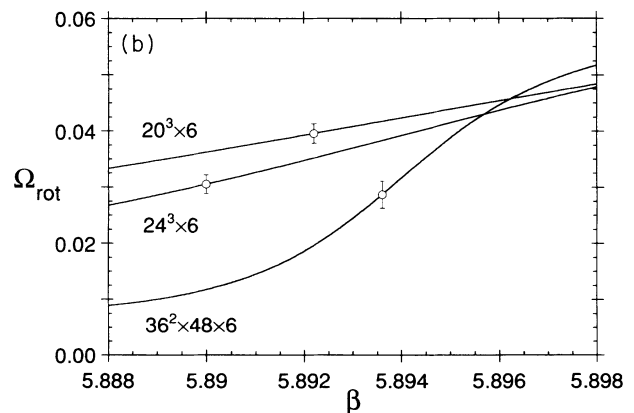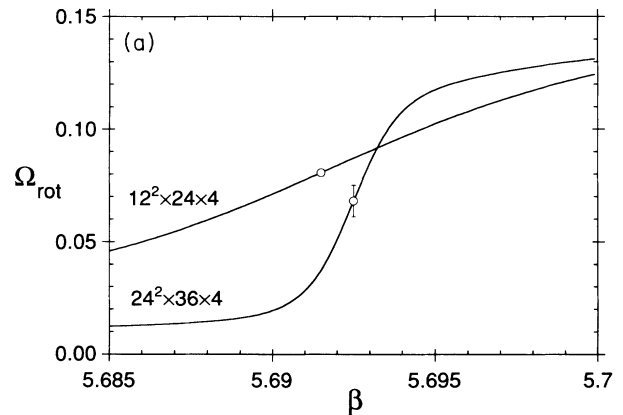The FSS theory predicts a scaling law

FIG. 7. The average of the $Z(3)$-rotated Polyakov loop $\langle \Omega_{\text{rot}} \rangle$. The solid lines are the results of the spectral density method: (a) $N_t = 4$, (b) $N_t = 6$.
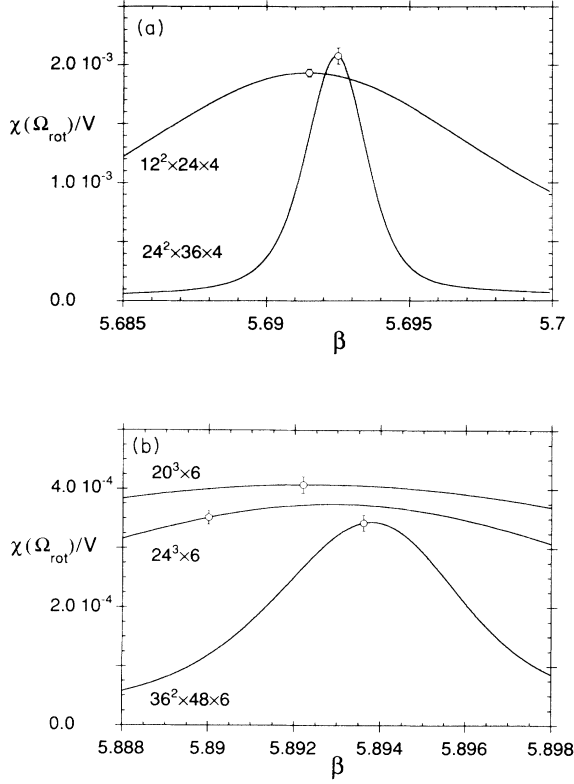
FIG. 8. The same as Fig. 6 for the normalized susceptibility $\chi(\Omega_{\mathrm{rot}})/V$.

$$\chi_{\max}(V) \sim V^{\rho} , \tag{4.1}$$

$$\beta_c(N_t,V) - \beta_c(N_t,\infty) \sim V^{-\sigma} , \tag{4.2}$$

with $\rho = \sigma = 1$ for the first-order transitions [18], in contrast with nontrivial critical exponents of second-order transitions. As a typical example, the second-order deconfining transition of the SU(2) gauge theory is characterized by $\rho = 0.64(1)$ and $\sigma = 0.51(3)$ [19].

The V dependence of $\chi_{\max}(\Omega_{\mathrm{rot}})$ and $\chi_{\max}(P)$ is summarized in Figs. 10 and 11, respectively, together with the results of other collaborations for $N_t = 4$ [4,5]. The linear V dependence of the $N_t = 4$ data confirms the first-order nature of the transition. Our results for $N_t = 4$ are consistent with the scaling line of the previous results. Our new data for $N_t = 6$ also show a clear linearity. The re-
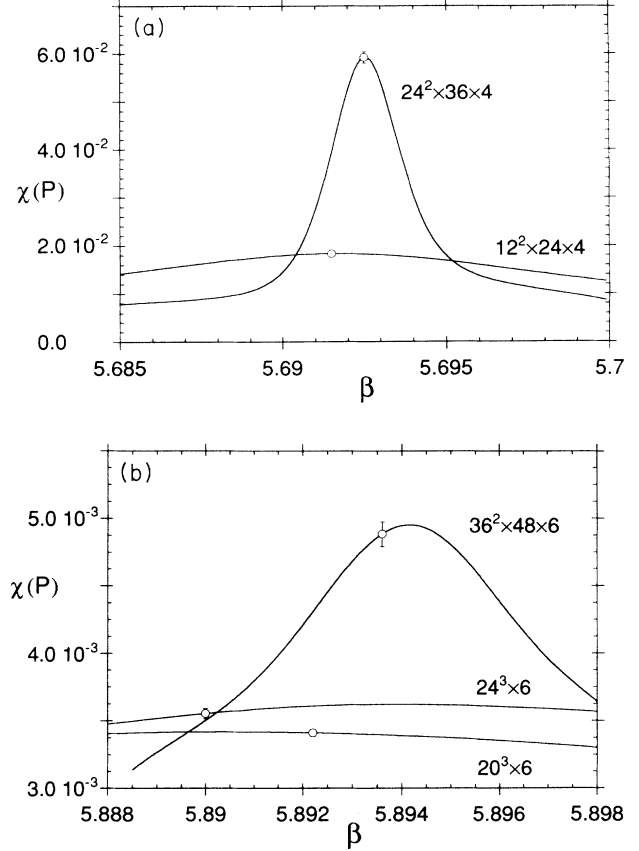

FIG. 9. The same as Fig. 6 for the susceptibility $\chi(P)$.

sults of our scaling fits for $\chi_{\max}(\Omega_{\mathrm{rot}})$ are summarized in Table III. For the fit of $N_t = 4$ results, we have included the data of other groups [4,5]. The fits here and in the following are done with SALS program system [20]. We find the critical exponent ρ to be very close to unity. The results for $\chi_{\max}(P)$ are similar with larger error bars. We find $\chi_{\max}(P) = 0.011(3) + 0.00025(21) \times (V/N_t^3)^{0.92(14)}$ for $N_t = 4$, $V = 16^3 - 28^3$, and $\chi_{\max}(P) = 0.0031(4) + 0.00002(+10/-2) \times (V/N_t^3)^{0.80(35)}$ for $N_t = 6$, $V = 20^3 - 36^2 \times 48$. Thus the result for $N_t = 6$ also confirms the previous conclusion obtained for $N_t = 4$ [1] that the deconfining transition is of first order.

The value of β_c at $V = \infty$ is determined by (4.2) by

TABLE II. Peak height and peak position of the susceptibilities obtained by the spectrum density method. Errors are estimated by the jackknife method.

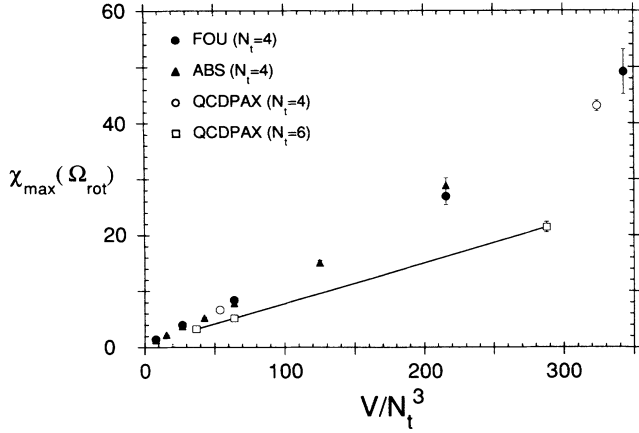| Lattice	$24^2 \times 36 \times 4$	$12^2 \times 24 \times 4$	$36^2 \times 48 \times 6$	$24^3 \times 6$	$20^3 \times 6$
$\chi_{\max}(\Omega_{\mathrm{rot}})/V$	$2.082(46) \times 10^{-3}$	$1.935(34) \times 10^{-3}$	$3.44(15) \times 10^{-4}$	$3.74(16) \times 10^{-4}$	$4.08(14) \times 10^{-4}$
$\chi_{\max}(P)/V$	$2.858(65) \times 10^{-6}$	$5.306(64) \times 10^{-6}$	$7.96(15) \times 10^{-8}$	$2.620(44) \times 10^{-7}$	$4.275(35) \times 10^{-7}$
$\chi_{\max}(P_t - P_s)/V$			$4.4535(68) \times 10^{-8}$	$2.07(45) \times 10^{-7}$	$3.40(39) \times 10^{-7}$
$\beta_c(\Omega_{\mathrm{rot}})$	$5.69245(23)$	$5.69149(42)$	$5.89379(34)$	$5.89292(87)$	$5.8924(14)$
$\beta_c(P)$	$5.69254(20)$	$5.69164(31)$	$5.89416(33)$	$5.8938(52)$	$5.8903(13)$
$\beta_c(P_t - P_s)$			$5.89448(52)$	$5.871(22)$	$5.891(29)$

FIG. 10. $\chi_{max}(\Omega_{rot})$ as a function of relative spatial volume V/N_t^3.

fixing $\sigma = 1$. The V^{-1} dependence of β_c is shown in Figs. 12 and 13, the results of the fit being summarized in Table IV. The fit is stable under a variation of the fit range, and the β_c's obtained both by the $\chi(\Omega_{rot})$ and the $\chi(P)$ are consistent with each other. We estimate

$$\beta_c(N_t = 4 \, , \ V = \infty) = 5.692\,54(24) \tag{4.3}$$

from the fit of β_c obtained by $\chi(\Omega_{rot})$ using $V = 16^3 - 28^3$ and

$$\beta_c(N_t = 6 \, , \ V = \infty) = 5.894\,05(51) \tag{4.4}$$

using $V = 24^3 - 36^2 \times 48$. We note that the value of the coefficient $C(N_t)$ in Table IV is independent of N_t within the errors, suggesting that the leading FSS is determined by the relative volume V/N_t^3 alone.

Our estimate of $\beta_c(4, \infty)$ is consistent with the estimate of Fukugita, Okawa, and Ukawa [4], 5.69226(41) $(V = 16^3 - 28^3)$, and Alves, Berg, and Sanielevici [5], 5.6923(7) $(V = 14^3 - 24^3)$. However, it is slightly larger than that of the latter group including the data of smaller lattices: 5.6910(4) $(V = 8^3 - 24^3)$. Note also that there is a
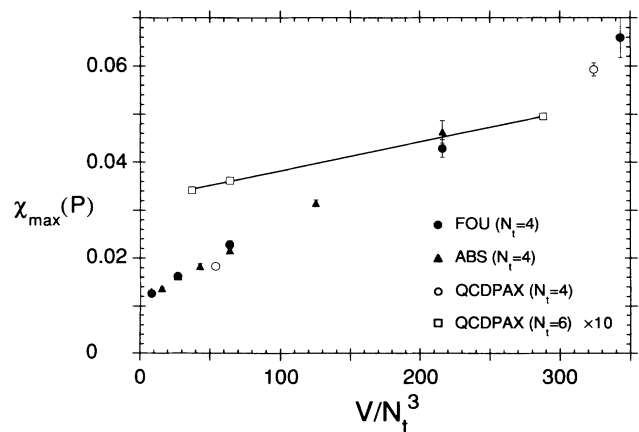

FIG. 11. The same as Fig. 10 for $\chi_{max}(P)$. The value of $\chi_{max}(P)$ for $N_t = 6$ is multiplied by a factor of 10.
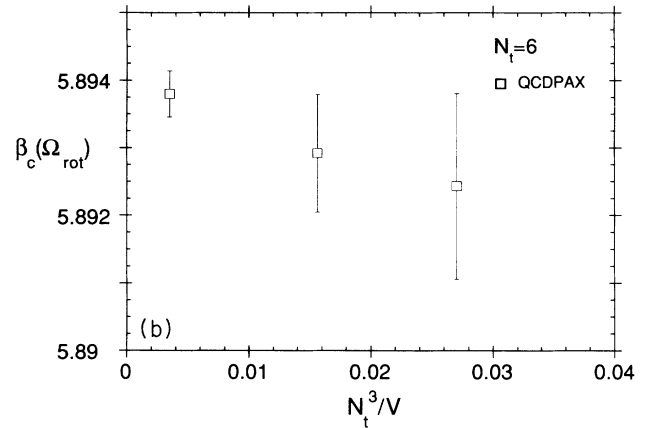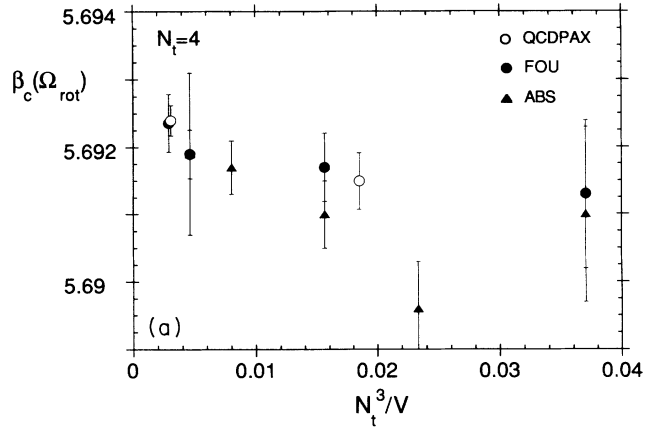

FIG. 12. β_c determined by $\chi(\Omega_{rot})$: (a) $N_t = 4$, (b) $N_t = 6$.

sizable systematic difference between the value of $\beta_c(N_t, V)$ determined from $\chi(\Omega_{rot})$ and that from $\chi(P)$ on small lattices such as $V = 8^3$ and 10^3 [4,5]. Our $\beta_c(6, \infty)$ is significantly larger than a previous estimate [21] of 5.877(6) extrapolated from small lattices: $V = 7^3 - 11^3$.

Comparing the N_t dependence of our $\beta_c(N_t, \infty)$ with the prediction of the two-loop perturbation theory for the shift of β_c, $\Delta\beta_{2\,loop}$ we find $[\beta_c(6, \infty) - \beta_c(4, \infty)] / \Delta\beta_{2\,loop} = 0.561(2)$. This asymptotic-scaling violation was noted in previous works [21] and the magnitude of the violation is consistent with previous estimates by the Monte Carlo renormalization group (MCRG) method at these β's [22].

V. LATENT HEAT

Now we study gaps of thermodynamic quantities at the phase transition, in particular the energy density ϵ and the pressure p (in dimensionless form):

$$\epsilon \equiv \frac{a^4}{V_s} \frac{\partial}{\partial(1/T)} \ln Z(T) \, ,$$

$$p \equiv \frac{a^4}{1/T} \frac{\partial}{\partial V_s} \ln Z(T) \, , \tag{5.1}$$
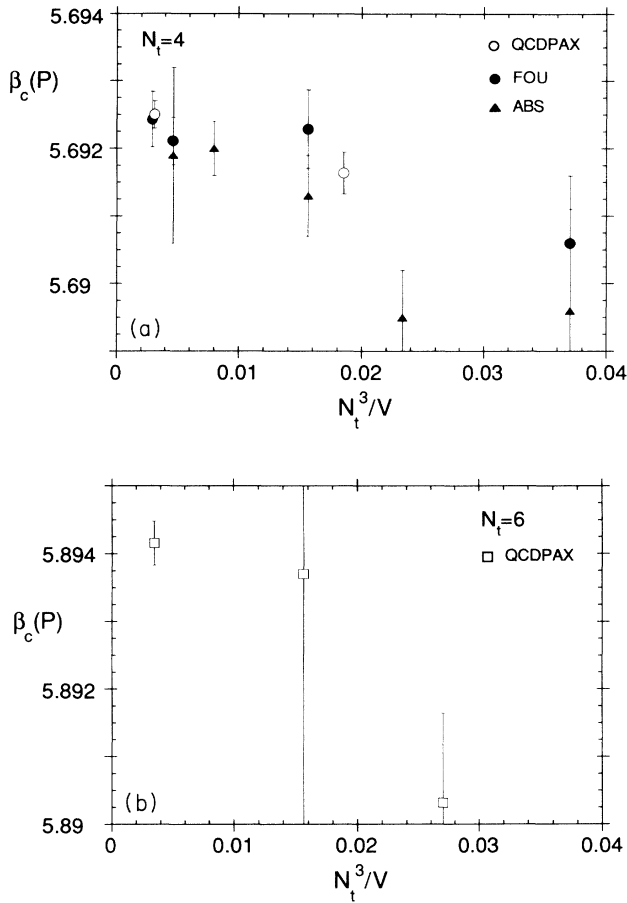
FIG. 13. The same as Fig. 12 for β_c determined by $\chi(P)$.

$$\epsilon - 3p = -36\frac{\tilde{\beta}(g)}{g^3}(P_t + P_s) \ ,$$

$$\epsilon + p = 4\beta\tilde{c}(\beta)(P_t - P_s) \ . \tag{5.2}$$

Here $\tilde{\beta}(q)$ is the renormalization-group β function and $\tilde{c}(\beta)$ is a response function of the gauge coupling constant with respect to an anisotropic deformation of the lattice [24]. In the one-loop perturbation theory, they are given by [23] $\tilde{\beta}(g)/g^3 = -11/4\pi^2 + O(\beta^{-1})$, and $\tilde{c}(\beta) = 1 - 1.000\,62\beta^{-1} + O(\beta^{-2})$. (Strictly speaking, the $\epsilon - 3p$ requires a further subtraction of the zero-temperature contribution [23]. In the gap studied in the following, however, this contribution cancels out.)

To estimate the gaps of these quantities, we separate our Monte Carlo runs at the transition point into two phases. As shown in the proceeding sections, on our large lattices ($24^2 \times 36 \times 4$ and $36^2 \times 48 \times 6$), our β's locate exactly at the transition point and the two-phase structure is very clear both in the history and in the histogram.

We first try to separate the runs by imposing cuts to Ω_{rot} or $|\Omega|$. We find, however, the resulting expectation values are sensitive to the choice of the value of the cut, and it is difficult to get an unambiguous result, as noted in [4]. We instead separate the runs by inspecting the time history of the Polyakov loop. A sufficient number of iterations around flip-flops and around spikes should be removed to avoid contamination from transition stages [4]. Figure 14 is an example of expectation values of observables in each phase as a function of the number of removed iterations. In this example, 3000 iterations have to be removed to obtain a stable and unambiguous result. We disregard 3000 (2000) iterations around the flip-flops and spikes for $36^2 \times 48 \times 6$ ($24^2 \times 36 \times 4$) lattice. Only when the average persistence time of each phase is sufficiently large compared with that of the transition stage are we able to obtain stable results: This condition is satisfied only on spatially large lattices. On the

where $V_s = a^3 V$ and $1/T = aN_t$ on isotropic lattices. Conventionally, the combinations of $\epsilon - 3p$ and $\epsilon + p$ are studied, because they are proportional to a sum and a difference of P_t and P_s, respectively [23]:

TABLE III. Finite-size scaling fits for $\chi_{\text{max}}(\Omega_{\text{rot}})$. For $N_t = 4$, the data of Refs. [4] and [5] are included in the fit. The fit with D_2 and ρ_2 is done for comparison with previous results given in the literature.

N_t	V	$\chi(N_t, V) = \chi(N_t, 0) + D(N_t)(V/N_t^3)^{\rho(N_t)}$		
		$\chi(N_t, 0)$	$D(N_t)$	$\rho(N_t)$
4	$12^3 - 28^3$	1.54(26)	0.048(09)	1.171(34)
	$14^3 - 28^3$	0.93(69)	0.067(25)	1.115(63)
	$12^2 \times 24 - 28^3$	1.53(81)	0.050(23)	1.164(77)
	$16^3 - 28^3$	2.37(1.10)	0.036(21)	1.122(98)
6	$20^3 - 36^2 \times 48$	0.69(84)	0.065(54)	1.017(135)

N_t	V	$\chi(N_t, V) = \chi_1(N_t, 0) + D_1(N_t)(V/N_t^3)$ $\chi(N_t, V) = D_2(N_t)(V/N_t^3)^{\rho_2(N_t)}$			
		$\chi_1(N_t, 0)$	$D_1(N_t)$	$D_2(N_t)$	$\rho_2(N_t)$
4	$12^3 - 28^3$	0.19(23)	0.1249(43)	0.126(13)	1.004(23)
	$14^3 - 28^3$	$-0.47(20)$	0.1321(30)	0.105(66)	1.039(13)
	$12^2 \times 24 - 28^3$	$-0.48(25)$	0.1322(34)	0.106(77)	1.039(15)
	$16^3 - 28^3$	$-0.61(45)$	0.1329(41)	0.101(13)	1.047(24)
6	$20^3 - 36^2 \times 48$	0.58(19)	0.0722(36)	0.116(14)	0.921(27)
	$24^3 - 36^2 \times 48$	0.53(40)	0.0726(43)	0.102(25)	0.945(42)

TABLE IV. Finite-size scaling fit of β_c obtained by the Ω_{rot} and P susceptibilities: $\beta_c(N_t,V)=\beta_c(N_t,\infty)-C(N_t)(N_t^3/V)$.

N_t	V	Ω_{rot} $\beta_c(N_t,\infty)$	$C(N_t)$	P $\beta_c(N_t,\infty)$	$C(N_t)$
4	12^3-28^3	5.692 43(20)	0.064(17)	5.692 65(19)	0.069(16)
	14^3-28^3	5.692 56(22)	0.084(21)	5.692 67(21)	0.072(20)
	$12^2\times24-28^3$	5.692 47(22)	0.065(24)	5.692 56(20)	0.051(21)
	16^3-28^3	5.692 54(24)	0.082(32)	5.692 58(23)	0.056(35)
6	$20^3-36^2\times48$	5.894 01(44)	0.063(49)	5.894 72(42)	0.161(58)
	$24^3-36^2\times48$	5.894 05(51)	0.072(77)	5.894 29(153)	0.038(425)

$36^2\times48\times6(24^2\times36\times4)$ lattice, the average number of iterations between flip-flops and spikes is about 16 000(19 000). On our small lattices the above condition is not satisfied and therefore we are unable to obtain stable results on these lattices. Our results for $(\epsilon-3p)/T^4$ and $(\epsilon+p)/T^4$ on the large lattices are summarized in Table V.

At a first-order transition, the coefficient of leading FSS of $\chi_{max}(P)$ is related to the plaquette gap for $V=\infty$ [18]. This provides us with another way of estimating $\Delta(\epsilon-3p)/T^4$ [5]. The results of our FSS fit to the data shown in Fig. 11 are given in Table VI. We find that the result for $N_t=4$ agrees completely with our direct measurement on the $24^2\times36\times4$ lattice given in Table V. The result for $N_t=6$ is also consistent with our direct measurement on the $36^2\times48\times6$ lattice. The slightly (two standard deviation) smaller values for $\Delta(\epsilon-3p)/T^4$ obtained by the FSS fit for $N_t=6$ can be understood as due to either of the following: (1) the values of V used for the FSS fit are not sufficiently large to extract the $V=\infty$ limit, or (2) the gap is still slowly decreasing with V on the $36^2\times48\times6$ lattice. Identifying the origin of the slight difference among these two possibilities is beyond the scope of the present study.

These results can be compared with the previous ones: on the $24^3\times4$ lattice at the same β, $\Delta(\epsilon-3p)/T^4=4.200(95)$ (Fukugita, Okawa, and Ukawa [4]); 3.78(20) (Brown et al. [2]), and $\Delta(\epsilon+p)/T^4=2.927(97)$ (Fukugita, Okawa, and Ukawa); 2.54(12)

FIG. 14. The average of $(\epsilon-3p)/T^4$ in each phase on the $36^2\times48\times6$ lattice as a function of the number of removed iterations near each flip-flop and spike.

(Brown et al.). On the $28^3\times4$ lattice at $\beta=5.692$, $\Delta(\epsilon-3p)/T^4=4.11(12)$ and $\Delta(\epsilon+p)/T^4=2.826(37)$ (Fukugita, Okawa, and Ukawa). Our results for $N_t=4$ are completely consistent with those by Fukugita, Okawa and Ukawa. We find that the values of the physical quantities in both phases themselves agree with each other.

For $N_t=6$, Brown et al. estimated [2] $\Delta(\epsilon+p)/T^4=2.48(24)$ on a $24^3\times6$ lattice. We find a much smaller value, 1.835(51), for this gap. Our results of $(\epsilon+p)/T^4$ for $N_t=6$ is shown in Fig. 15 together with the data of Brown et al. [25]. Consulting this figure, we understand the origin of the discrepancy as follows: (1) Brown et al. measured $(\epsilon+p)/T^4$ in the deconfined phase at $\beta=5.9$ which is slightly above our estimate of β_c and obtained [25] 2.60(22) which is larger than our value 2.195(37) at $\beta=5.8936$ by 0.41. This difference can be attributed to the sharp drop in $(\epsilon+p)/T^4$ above the transition point. (2) The value of $(\epsilon+p)/T^4$ in the confined phase assumed by Brown et al. [25] is 0.12(10) at $\beta=5.875$ which is smaller than our value 0.360(35) by 0.24. Our data indicates that the increase of $(\epsilon+p)/T^4$ in the confined phase near β_c in the data of Brown et al., which they took to be due to mixing of the phases and disregarded in the estimation, is partly a real effect. Thus these two facts in total lead to the difference of 0.65 for the gap. We note that in the paper [2] of Brown et al. they pointed out themselves the possibility of a slight overestimate of the latent heat.

These results for the latent heat raise two problems. First, gaps for $N_t=6$ are smaller than those for $N_t=4$ by a factor 1.5 for $\Delta(\epsilon+p)$ and 1.7 for $\Delta(\epsilon-3p)$, indicating
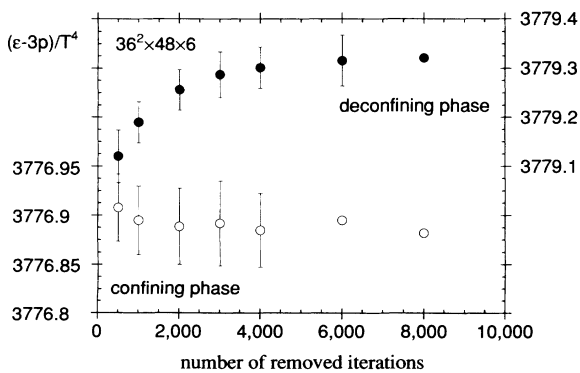
TABLE V. $(\epsilon-3p)/T^4$ and $(\epsilon+p)/T^4$ with one-loop perturbative coefficients assumed. Phase separation is performed as explained in the text.

Lattice	$24^2\times36\times4$	$36^2\times48\times6$
β	5.6925	5.8936
$(\epsilon+p)_{had}/T^4$	0.551(47)	0.360(35)
$(\epsilon+p)_{QGP}/T^4$	3.324(29)	2.195(37)
$(\epsilon-3p)_{had}/T^4$	703.478(74)	3776.892(43)
$(\epsilon-3p)_{QGP}/T^4$	707.539(42)	3779.287(46)
$\Delta(\epsilon+p)/T^4$	2.773(55)	1.835(51)
$\Delta(\epsilon-3p)/T^4$	4.062(85)	2.395(63)

TABLE VI. Finite-size scaling fit for $\chi_{max}(P)$ assuming a first-order phase transition: $\chi(N_t,V)=\chi(N_t,0)+D(N_t)(V/N_t^3)$. For $N_t=4$, the data given in Refs. [4] and [5] are included in the fit. $\Delta(\epsilon-3p)/T^4$ is determined by the plaquette gap defined by $\Delta P=2[D(N_t)/N_t^3]^{1/2}$. The one-loop expression for the coefficient $\tilde{c}(\beta)$ is assumed.

N_t	V	$\chi(N_t,0)$	$D(N_t)$	$\Delta(\epsilon-3p)/T^4$
4	12^3-28^3	$1.137(57)\times10^{-2}$	$1.485(82)\times10^{-4}$	$3.911(11)$
	14^3-28^3	$1.054(66)\times10^{-2}$	$1.556(82)\times10^{-4}$	$4.005(11)$
	$12^2\times24-28^3$	$1.029(70)\times10^{-2}$	$1.572(83)\times10^{-4}$	$4.025(11)$
	16^3-28^3	$1.279(64)\times10^{-2}$	$1.455(48)\times10^{-4}$	$3.872(64)$
6	$20^3-36^2\times48$	$3.200(32)\times10^{-3}$	$6.10(31)\times10^{-6}$	$2.185(55)$
	$24^3-36^2\times48$	$3.241(81)\times10^{-3}$	$5.94(42)\times10^{-6}$	$2.155(153)$

naively a scaling violation at $\beta\simeq5.7-5.9$. Second, both $N_t=4$ and $N_t=6$ results show discrepancies between the values $\Delta(\epsilon-3p)$ and $\Delta(\epsilon+p)$, which naively suggests a finite pressure gap at the transition, although it becomes smaller for a larger N_t.

Since the violation of the asymptotic scaling at these β's is already well established, the use of perturbative coefficients for $\epsilon-3p$ and $\epsilon+p$ is not validated and we have to estimate nonperturbative corrections to these quantities.

MCRG studies show that, although the asymptotic scaling is violated for $\beta<6$, several quantities obey, roughly speaking, a common effective scaling law if β is not too small [22]. Since the coefficient of $\epsilon-3p$ is given by the β function, we can use the nonperturbative β function of the MCRG studies for a nonperturbative estimate of the $\epsilon-3p$. The correction factor to the one-loop perturbative β function which the MCRG studies [22] give is 0.6 ± 0.05 at $\beta\simeq5.7$ and 0.75 ± 0.07 at $\beta\simeq5.9$. Large error bars are caused by the dispersive MCRG results. (A similar approach was proposed also by Engels *et al.* [26].)
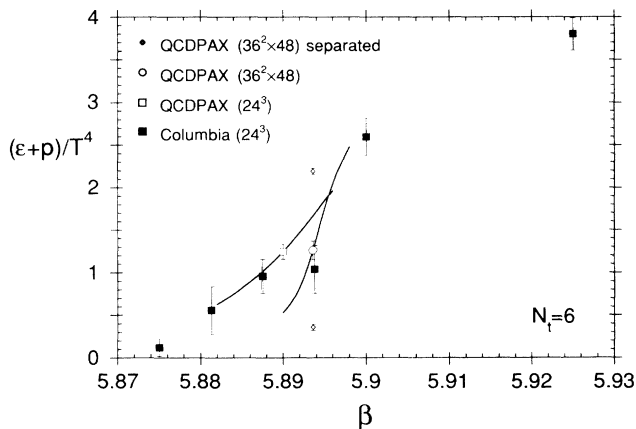

FIG. 15. $(\epsilon+p)/T^4$ for $N_t=6$ near the transition point. Small diamonds show the expectation value of $(\epsilon+p)/T^4$ in each phase on the $36^2\times48\times6$ lattice. Phase separation is performed as explained in the text. The solid lines are the results obtained by the spectral density method using our data.

These corrections make $\Delta(\epsilon-3p)/T^4=2.44(24)$ for $N_t=4$ and $1.80(18)$ for $N_t=6$ [27]. Therefore even after we include the correction factors, the discrepancy between the two remains. Thus $\Delta(\epsilon-3p)/T^4$ shows a substantial scaling violation [28].

We now find the difference between the corrected $\Delta(\epsilon-3p)/T^4$ [2.44(24) for $N_t=4$ and 1.80(18) for $N_t=6$] and the uncorrected $\Delta(\epsilon+p)/T^4$ [2.77(6) for $N_t=4$ and 1.84(5) for $N_t=6$] is small for both $N_t=4$ and $N_t=6$. Since we expect a vanishing Δp, this suggests that the nonperturbative corrections to the coefficient of $\epsilon+p$ is small. Confirmation of this requires a nonperturbative study of anisotropic lattices [29] with a small anisotropy.

VI. CONCLUSION

We have performed a high-statistics measurement of the deconfining transition in the SU(3) gauge theory on the dedicated parallel computer QCDPAX. The first-order nature of the transition is confirmed by the linear FSS of susceptibilities both on $N_t=4$ and 6 lattices. On the spatially large lattices ($24^2\times36\times4$ and $36^2\times48\times6$), we have measured the gaps of the energy density and the pressure both by separating our Monte Carlo runs into two phases and by applying a FSS theory for the gap $\Delta(\epsilon-3p)$. The two results thus obtained are remarkably consistent with each other. We have found that the latent heat for $N_t=6$ is much smaller than that previously estimated on a spatially smaller lattice and also that for $N_t=4$. The latent heat we have found for $N_t=6$ is about $\frac{1}{3}$ of the Stefan-Boltzmann value $8\pi^2/15$.

[1] A. Ukawa, in *Lattice '89*, Proceedings of the International Symposium, Capri, Italy, 1989, edited by R. Petronzio *et al.* [Nucl. Phys. B (Proc. Suppl.) **17**, 118 (1990)].

[2] F. R. Brown *et al.*, Phys. Rev. Lett. **61**, 2058 (1988); F. R. Brown, in *Lattice '89* [1], p. 214.

[3] S. Cabasino *et al.*, in *Lattice '89* [1], p. 218.

[4] M. Fukugita, M. Okawa, and A. Ukawa, Phys. Rev. Lett. **63**, 1768 (1989); Nucl. Phys. **B337**, 181 (1990).

[5] N. A. Alves, B. A. Berg, and S. Sanielevici, Phys. Rev. Lett. **64**, 3107 (1990); Nucl. Phys. **B376**, 218 (1992).

[6] Y. Iwasaki *et al.*, in *Lattice '90*, Proceedings of the International Symposium, Tallahassee, Florida, 1990, edited by U. M. Heller, A. D. Kennedy, and S. Sanielevici [Nucl. Phys. B (Proc. Suppl.) **20**, 141 (1991)]; K. Kanaya *et al.*, *ibid.*, p. 300.

[7] Y. Iwasaki *et al.*, Phys. Rev. Lett. **67**, 3343 (1991); K. Kanaya *et al.*, in *Lattice '91*, Proceedings of the Internationa Symposium, Tsukuba, Japan, 1991, edited by M. Fukugita, Y. Iwasaki, M. Okawa, and A. Ukawa [Nucl. Phys. B (Proc. Suppl) **26**, 302 (1992)].

[8] Y. Iwasaki *et al.*, Comp. Phys. Commun. **49**, 449 (1988); T. Shirakawa *et al.*, in *Proceedings of Supercomputing '89*, Reno, 1989, edited by F. R. Baily, G. Johnson, and C. E. Oliver (The Association for Computing Machinery, New York, 1989), p. 495; Y. Iwasaki *et al.*, in *Lattice '89* [1], p. 259.

[9] T. Hoshino, *PAX Computer, High-Speed Parallel Processing and Scientific Computing* (Addison-Wesley, New York, 1989).

[10] N. Cabibbo and E. Marinari, Phys. Lett. **B119**, 387 (1982); M. Okawa, Phys. Rev. Lett. **49**, 353 (1982).

[11] S. Itoh, Y. Iwasaki, and T. Yoshié, Phys. Rev. D **33**, 1806 (1986).

[12] A. M. Polyakov, Phys. Lett. **72B**, 477 (1978); L. Susskind, Phys. Rev. D **20**, 2610 (1979).

[13] We find that almost all phase flips among the three $Z(3)$-broken phases occur only via the symmetric phase. This is reflected in the fact that the histogram of Ω does not show a raise on the path connecting directly the $Z(3)$-broken peaks.

[14] B. Svetitsky and L. G. Yaffe, Nucl. Phys. **B210** [FS6], 423 (1982); J. Polonyi and K. Szlachanyi, Phys. Lett. **110B**, 395 (1982).

[15] B. Efron, SIAM Rev. **21**, 460 (1979); R. G. Miller, Biometrica **61**, 1 (1974).

[16] S. Gottlieb *et al.*, Nucl. Phys. **B263**, 704 (1986).

[17] I. R. McDonald and K. Singer, Discuss. Faraday Soc. **43**, 40 (1967); A. M. Ferrenberg and R. Swendsen, Phys. Rev. Lett. **61**, 2058 (1988); **63**, 1195 (1989).

[18] Y. Imry, Phys. Rev. B **21**, 2042 (1980); M. E. Fisher and A. N. Baker, *ibid.* **26**, 2507 (1982); H. W. J. Blöte and M. P. Nightingale, Physica **112A**, 405 (1982); J. L. Cardy and P. Nightingale, Phys. Rev. B **27**, 4256 (1983); K. Binder and D. P. Landau, *ibid.* **30**, 1477 (1984); M. S. S. Challa, D. P. Landau, and K. Binder, *ibid.* **34**, 1841 (1986).

[19] J. Engels, J. Fingberg, and M. Weber, Nucl. Phys. **B332**, 737 (1990).

[20] T. Nakagawa and Y. Oyanagi, in *Recent Developments in Statistical Inference and Data Analysis*, edited by K. Matusita (North Holland, Amsterdam, 1980), pp. 221–225.

[21] A. D. Kennedy *et al.*, Phys. Rev. Lett. **54**, 87 (1985).

[22] A. Hasenfratz *et al.*, Phys. Lett. **140B**, 76 (1984); K. C. Bowler *et al.*, Nucl. Phys. **B257** [FS14], 155 (1985); A. D. Kennedy *et al.*, Phys. Lett. **155B**, 414 (1985); R. Gupta *et al.*, Phys. Lett. B **211**, 132 (1988); J. Hoek, Nucl. Phys. **B339**, 732 (1990).

[23] J. Engels *et al.*, Nucl. Phys. **B205** [FS5], 545 (1982); F. Karsh, *ibid.* **B205** [FS5], 285 (1982).

[24] The appearance of the β function can be easily understood by the definition (5.1), since the combination of $\epsilon - 3p$ is given by applying a uniform scale transformation $T^{-1}\partial/\partial T^{-1} + 3V_s\partial/\partial V_s$ to $\ln Z$.

[25] N. Christ (private communication).

[26] J. Engels *et al.*, Phys. Lett. B **252**, 625 (1990).

[27] In the first paper of Ref. [9] a wrong number is given for $N_t = 6$.

[28] Conversely, we can use $(\epsilon - 3p)/T^4$ to define another effective β function $\tilde{\beta}_{\text{eff}}$. We estimate $\tilde{\beta}_{\text{eff}}(\beta = 5.6915)/\tilde{\beta}_{\text{eff}}(\beta = 5.8922) = 0.621(13)$. This number should be compared with the perturbative value 1.056(1.053) for $\tilde{\beta}_{2(1)_{\text{loop}}}$ and with the value 0.8 ± 0.1 for $\tilde{\beta}_{\text{eff}}$ obtained by studies of MCRG and the deconfining phase transition [22]. Thus the $\Delta(\epsilon - 3p)/T_c^4$ does not scale in accord with the effective scaling obtained by the MCRG studies.

[29] G. Burger *et al.*, Nucl. Phys. **B304**, 587 (1988).